Bull. Mater. Sci., Vol. 15, No. 2, April 1992, pp. 131–141. © Printed in India.

Thermomechanical properties and microstructure of alumina-zirconia

B L MITRA, N C BISWAS and P S AGGARWAL
Central Glass and Ceramic Research Institute, Calcutta 700 032, India

MS received 28 August 1990; revised 30 April 1991

Abstract. Al_2O_3–ZrO_2 composites were prepared in two compositional ranges, 15 wt% ZrO_2 and 29 wt% ZrO_2 with or without yttria or magnesia stabilizers. While 1·5 wt% Y_2O_3 produced tetragonal ZrO_2 and fine grain microstructure, the 4·5 wt% Y_2O_3 developed cubic and tetragonal ZrO_2 with similar microstructure. Al_2O_3 with 29·5 wt% ZrO_2–1·5 wt% Y_2O_3 composition had the highest strength (3,300 kg/cm^2). The bending strength remained more or less the same after the first thermal shock, and then it decreased gradually, but retained some strength after 20 cycles of quench. The load vs displacement curve became nonlinear after thermal shock possibly because of formation of microcracks which could be seen by microstructural studies.

Keywords. Alumina-zirconia composites; thermal shock resistance; microcracks; inelasticity.

1. Introduction

It is well-known that dispersion of zirconia in alumina substantially improves its strength (Hori *et al* 1986; Marshall 1986; Lange and Miller 1987; Wang and Stevens 1988; Srinivasa Rao and Cannon 1989) and thermomechanical properties. The grain growth of alumina is also hindered by the addition of zirconia (Lange and Hirlinger 1984; Lin and Lu 1988), but the densification rate of alumina during sintering is reduced linearly with ZrO_2 addition (Majumdar *et al* 1986). The strengthening of alumina by zirconia depends on several factors. During stress-induced martensitic phase transformation of tetragonal zirconia particles to the monoclinic form, considerable stress is absorbed from the stress field of propagating cracks (Rühle *et al* 1986). The residual stresses around which already transformed monoclinic zirconia can cause microcracking and give further strengthening (Hori *et al* 1986). Cubic zirconia is also a toughening agent of alumina ceramics sintered in air (Kibbel and Heuer 1984). Crack deflection also plays an important role (Wang and Stevens 1988). Annealing at higher temperature (1200°C or above) gives rise to grain coarsening effect (Kibbel and Heuer 1986). The intergranular ZrO_2 particles appear to coarsen by coalescence as particles are dragged by migrating Al_2O_3 grain boundaries (Nettleship and Stevens 1987). This is controlled by ZrO_2–Al_2O_3 diffusion kinetics. The intragranular particles coarsen at a much slower rate (Kibbel and Heuer 1986). In general, Al_2O_3-ZrO_2 composites would often cope with appreciable thermal stresses. In the present work, the bending strength of as-fired, annealed and thermal-shocked samples of ZrO_2–Al_2O_3 composites containing 13·5 to 29 wt% ZrO_2 composites is compared. Microstructure and phase analysis of the composites are also presented.

Table 1. Batch composition, water absorption and bulk density.

Material wt%	Batch A	B	C	D	E
Al_2O_3	85·00	84·0	70·00	69·00	66·99
ZrO_2	15·00	14·50	29·00	29·50	28·64
Y_2O_3	—	1·50	—	1·50	4·37
MgO ($MgCO_3$)	—	—	1·0 (2·1)	—	—
Water absorption(%)	1·53	0·85	2·35	0·53	1·78
Bulk density (g/cc)	3·920	3·976	3·920	4·165	3·950
Theoretical density(%)	92·9	95·8	88·3	94·0	91·9

2. Experimental

Five compositions marked A, B, C, D, E (table 1) with stabilizing agents Y_2O_3 as well as MgO (batch C) in some cases were prepared by wet ball milling for 30 h. Bars of approximate dimensions 78 × 18 × 4–5 mm were made by dry-pressing at 650 kg/cm^2 followed by isostatic pressing at 3, 165 kg/cm^2 (45,000 psi). Two-step sintering combining 1 h isothermal heating at 1400°C and followed by 90 min soaking at 1560–1580°C was adopted. The fired sample surfaces were ground by 220 and 400 mesh SiC powders. The samples were annealed by heat treating the sample at 1140°C for 30 min before quenching. Thermal shock test was performed by thermal cycling the samples between 1200°C and drought-free air, giving at least 10 min soaking at 1200°C every time. Three-point bending strength and Young's modulus were determined by Instron. Fractured surfaces were etched by 15% HF–20% HCl mixed etchant and observed in scanning electron microscope (SEM). X-ray diffraction analysis (XDA) was carried out using Cu target. Bulk density was determined by the Archemedes method.

3. Results and discussion

The firing shrinkage of the samples averaged at 20–23%, a value, which was accounted for in making precision technical ceramics. Bulk density and water absorption values were recorded as shown in table 1. The use of yttria improved the density with respect to that obtained by the use of MgO additive (batch C). Small addition of MgO had a beneficial effect on sintering of Al_2O_3–ZrO_2 (Kosmac *et al* 1982) and acted as a stabilizer for ZrO_2 (Bansal and Heuer 1975; Zoz *et al* 1980). One MgO-composition of 1 wt% MgO was studied to get a good product.

By X-ray diffraction it was found that addition of Y_2O_3 increased tetragonal phase retention. The diffractogram traces for $(11\bar{1})$ *m*, (111) *t*, *c* and (111) *m* reflections were as shown in figure 1. The high angle diffraction for (400) *t*, (400) *c*, (004) *t* is as shown in figure 2. Composition B was almost free from monoclinic phase since (111) *m* reflection at 28·4° and $(11\bar{1})$ *m* reflection at 31·5° were found negligible. High angle

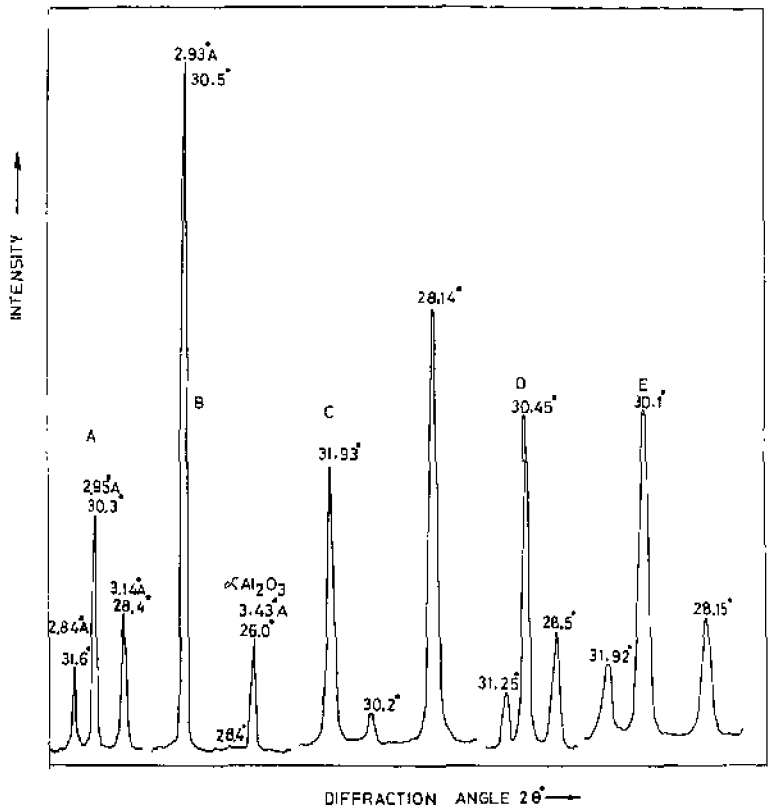

Figure 1. Low angle X-ray diffraction (peaks) diagrams.

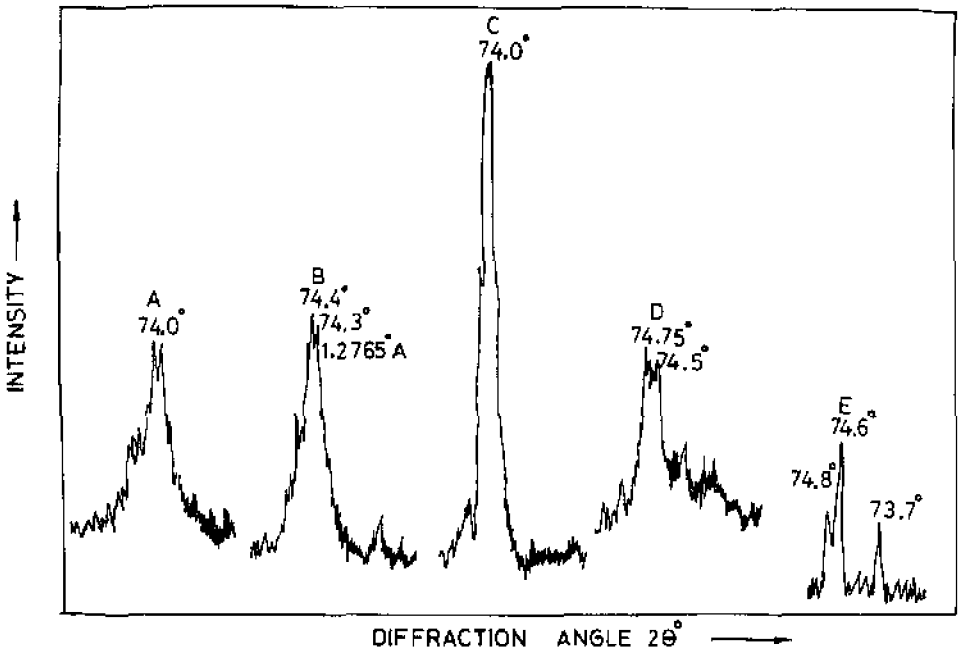

Figure 2. High angle X-ray diffraction (peaks) diagrams.

Table 2. Bending strength (in kg/cm^2) after different thermal cycling.

Batch	Samples as such	1 cycle thermal shock	3 cycles of thermal shock	5 cycles of thermal shock	10 cycles of thermal shock	15 cycles of thermal shock	20 cycles of thermal shock
A	2,250 ± 200	2,060 ± 200	560	570	520	—	404
B	2,960 ± 200	2,640 ± 200	712	600 ± 90	660	483	438
C	1,850 ± 300	1,890 ± 300	646	604	542	463	270
D	3,000 ± 300	3,290 ± 300	780	740	660	538	471
E	2,430 ± 200	2,350 ± 200	608	650	710	446	243

diffraction of sample B gave (400) reflection at 74·4° which according to Benedetti *et al* (1989) was for tetragonal ZrO_2. Other compositions (A, C, D, E) contained monoclinic zirconia, α-Al_2O_3 and another ZrO_2 phase. It was difficult to distinguish between tetragonal and cubic ZrO_2 from (111) reflection at 30·4°2θ. But from the high angle diffraction of figure 2, compositions A and C were found to contain cubic ZrO_2 (along with monoclinic ZrO_2). Composition D contained tetragonal along with monoclinic ZrO_2. Composition E developed tetragonal ZrO_2 (74·6°2θ), cubic ZrO_2 (73·7°2θ) and monoclinic ZrO_2 (28·15°2θ) together. The formation of cubic phase in A was probably due to the impurities from raw materials as well as from grinding the batches.

The three-point bending strength of unannealed samples was higher in the case of 15 wt% ZrO_2 batches and decreased considerably at 29 wt% ZrO_2 addition in batch C (table 2). But when 1·5 wt% Y_2O_3 was added to 29 wt% ZrO_2 batch, the highest strength was obtained. However when Y_2O_3 was increased to about 4·5%, the strength decreased. This could have been due to the formation of non-transformable cubic ZrO_2 in place of tetragonal ZrO_2 (Nettleship and Stevens 1987). The bending strength remained more or less the same after the first thermal shock, increased on first cycle in case of batches C and D, after that the strength decreased abruptly with increasing number of thermal shock cycling. This was evident from the results of third cycles. But even after 20 cycles of thermal shocks, these samples retained appreciable strength (240 to 470 kg/cm^2). Yuan *et al* (1986) reported lower strength of zirconia-mullite on thermal cycling (after 3 thermal shocks 460–1000 kg/cm^2). However, in our case, the load vs displacement curve was found to be nonlinear, especially after thermal shock cycling (figures 3a–e). The plastic deformation and the nature of the curves after thermal shock treatment suggested that microcracks were formed in the samples due to thermal shock and these microcracks were absorbing some amount of stress giving rise to plasticity.

Nonlinear stress-strain behaviour and plastic deformation in transformation-toughened materials have also been discussed by several workers (Marshall 1986; Matsui *et al* 1986; Heuer *et al* 1986; Swain 1990; Wu and Chen 1990). The pseudoplastic behaviour in these materials possibly arises both from stress-induced martensitic transformation as well as microcracking. Marshall (1986) observed linear stress-strain

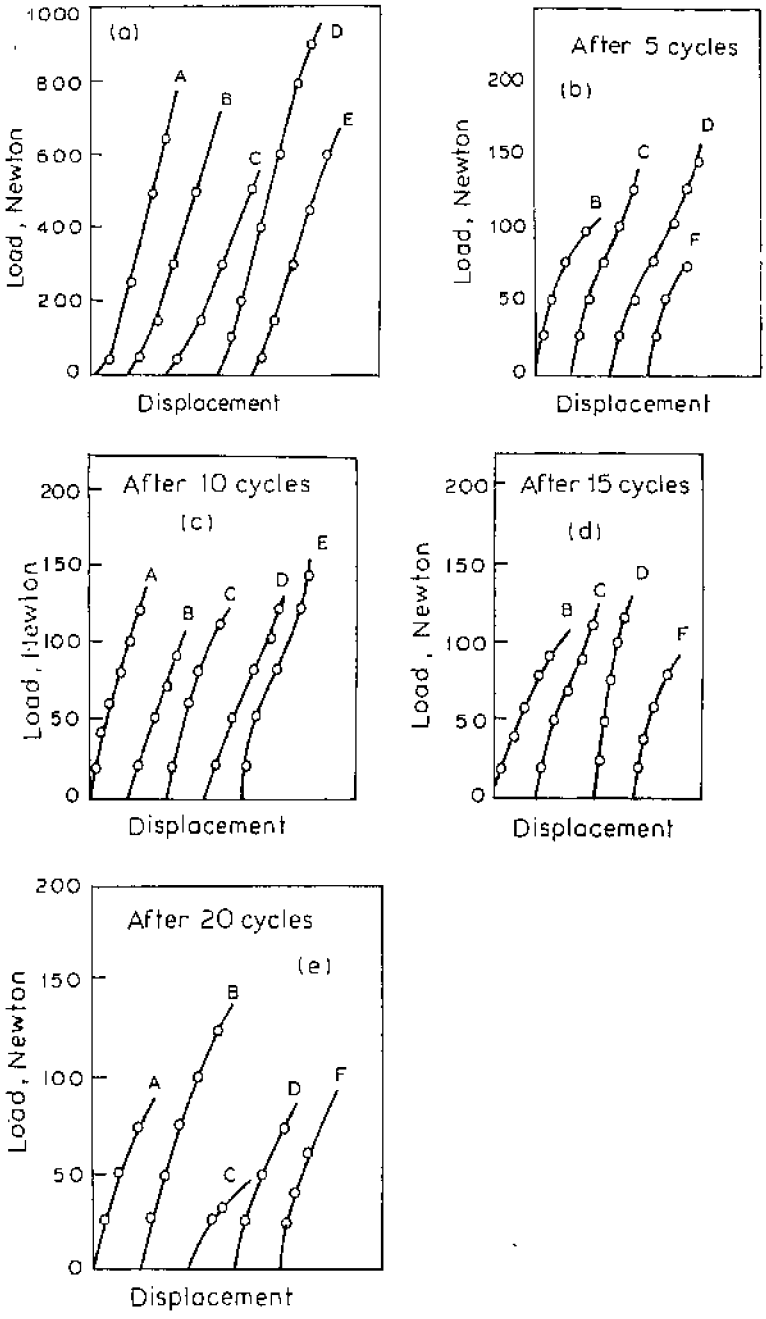

Figure 3. Load-displacement curves on flexural bending.

behaviour in overaged material, whereas nonlinear behaviour was seen in the toughened material. The increasing nonlinear component was evident at higher strains.

Young's modulus (E) was determined from the load displacement curve of 3-point bending test, from the following equations,

$$E = Wl^3/48\,I\delta, \tag{1}$$

Table 3. Young's modulus (in $\times 10^6$ kg/cm^2) after different thermal cycling.

Batch	Sample as such	Annealed 1 cycle	3 cycles of thermal shock	5 cycles of thermal shock	10 cycles of thermal shock	15 cycles of thermal shock	20 cycles of thermal shock
A	1·64	1·45	0·8	0·7	0·5	—	0·80
B	2·00	1·95	1·2	1·2	0·7	0·80	0·83
C	1·33	0·97	0·7	0·65	0·4	0·43	0·50
D	1·50	0·98	0·75	0·6	0·5	0·81	0·52
E	1·30	0·95	0·65	0·6	0·5	0·80	0·47

where the moment of inertia,

$$I = bt^3/12, \tag{2}$$

and deflection

$$\delta = \frac{a \times 2\,\text{mm}}{\text{Chart drive}} \times \text{cross head speed}. \tag{3}$$

Here W is load, l the span, b the breadth, t the thickness and a = chart reading corresponding to W.

Batches A and B had higher Young's modulus than batches C, D and E, although the strength of the composition *D* was the highest. This was probably because batches A and B contained higher quantities of alumina which was more elastic than ZrO_2. Young's modulus decreased on thermal shock treatment but started increasing after 15 cycles. Intergranular pores and cracks relaxed residual stresses (Buresh 1984). The reduction in E was indicative of considerable microcrack development (Swain 1990) on thermal shock. The rise of E after 15 cycles could have been due to the resistance to crack-growth by network of microcracks developed.

The scanning electron micrographs (SEM) of fractured surfaces are shown in figure 4(a) to 4(f). Figures 4a and 4b are fractographs of batches A and B prepared from ball-milled alumina and hence the grains are of bigger sizes. The remaining figures are those of samples made from vibro-energy-milled alumina which is much finer than ball-milled alumina. Grain size and pore sizes were much smaller in these cases. It was difficult to distinguish between alumina and zirconia grains in scanning electron micrographs without back scattering. But from XRD analysis and by comparison with the reported microstructure of other workers (Heuer *et al* 1982; Kibbel and Heuer 1986), small round and irregular-shaped grains were considered as zirconia. Intergranular zirconia crystallites as well as few intragranular ZrO_2 phase were seen enmeshed in Al_2O_3 crystals. The surrounding Al_2O_3 grains exert matrix constraint upon ZrO_2 grains thereby reducing the tendency of ZrO_2 grains to transform. At higher magnification (figure 2d), intragranular precipitates are revealed as engraved within the Al_2O_3 crystallites. In the micrographs of batches B and D, strong grain-to-grain bonding took place as a result of good sintering. The grain size of alumina was comparatively smaller in Y_2O_3 containing batches B (average 3·45 μm, pot milled batch) and D (average 1·76 μm, vibro energy-milled batch). The average grain size of Al_2O_3 in batch A was 7·3 μm (pot-milled batch) and in batch C, 2·7 μm (Vibro energy-milled batch), yttria had more pronounced grain growth retarding effect

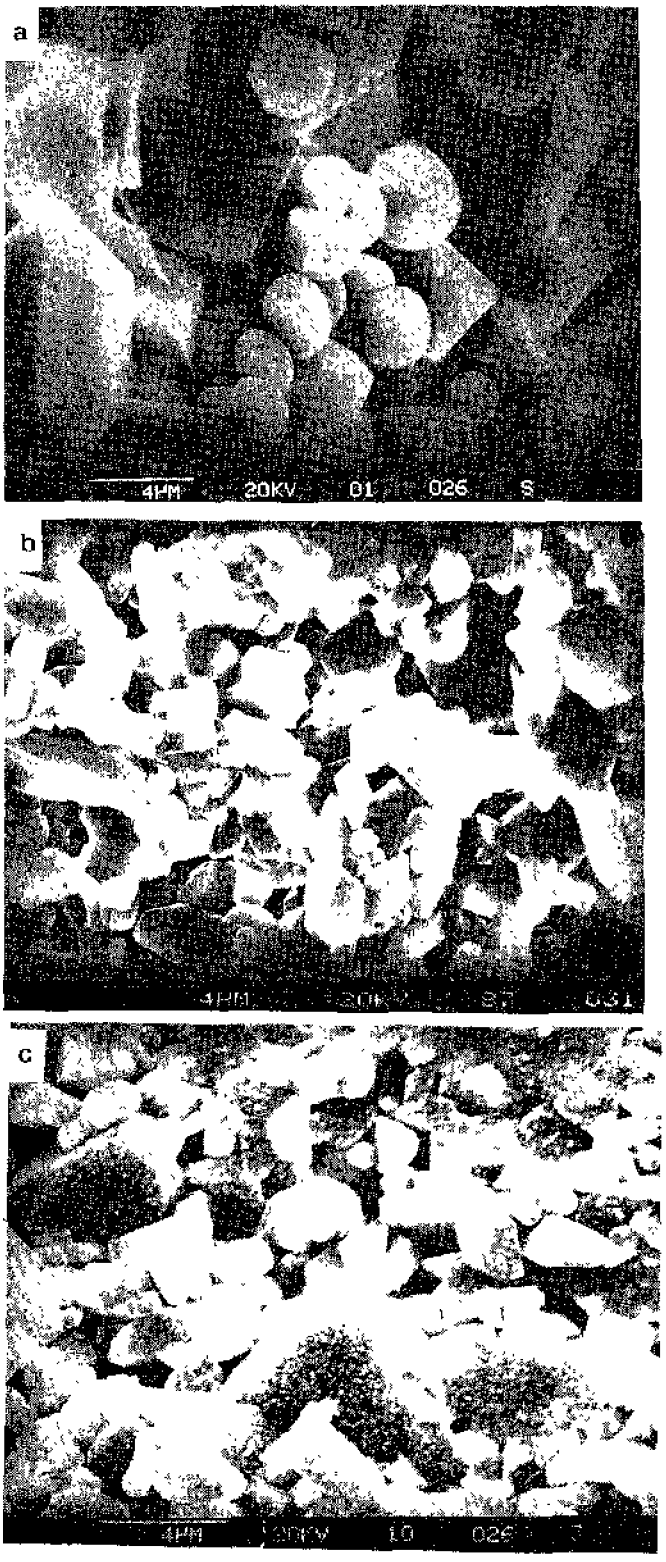

Figure 4(a–c). For caption, see p. 138.

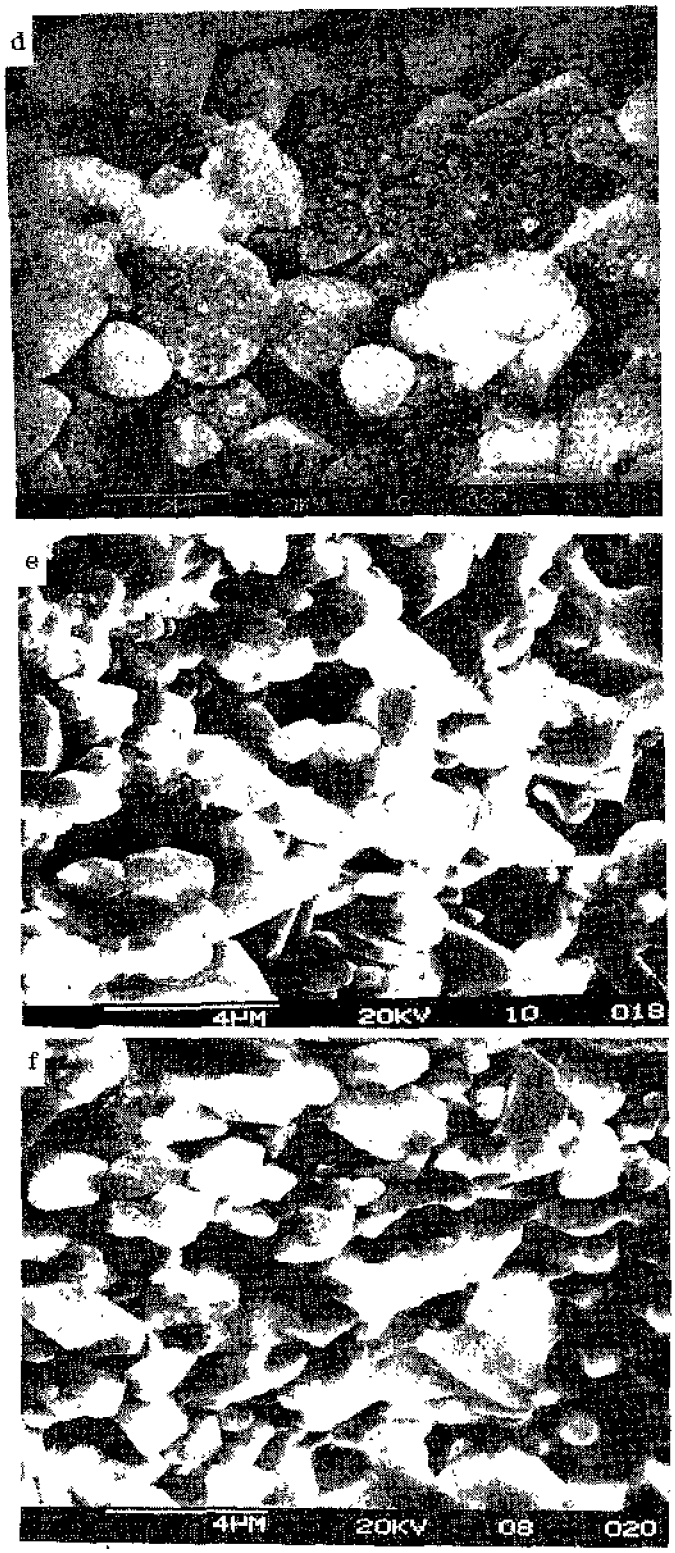

Figure 4. SEM fractographs. **a.** Composition A from ball-milled alumina, **b.** Composition B from ball-milled alumina, **c.** Composition C from vibro-energy milled Al_2O_3, **d.** Composition C with higher magnification, **e.** Composition D from vibro-energy milled Al_2O_3 and f. Composition E from vibro-energy milled Al_2O_3.

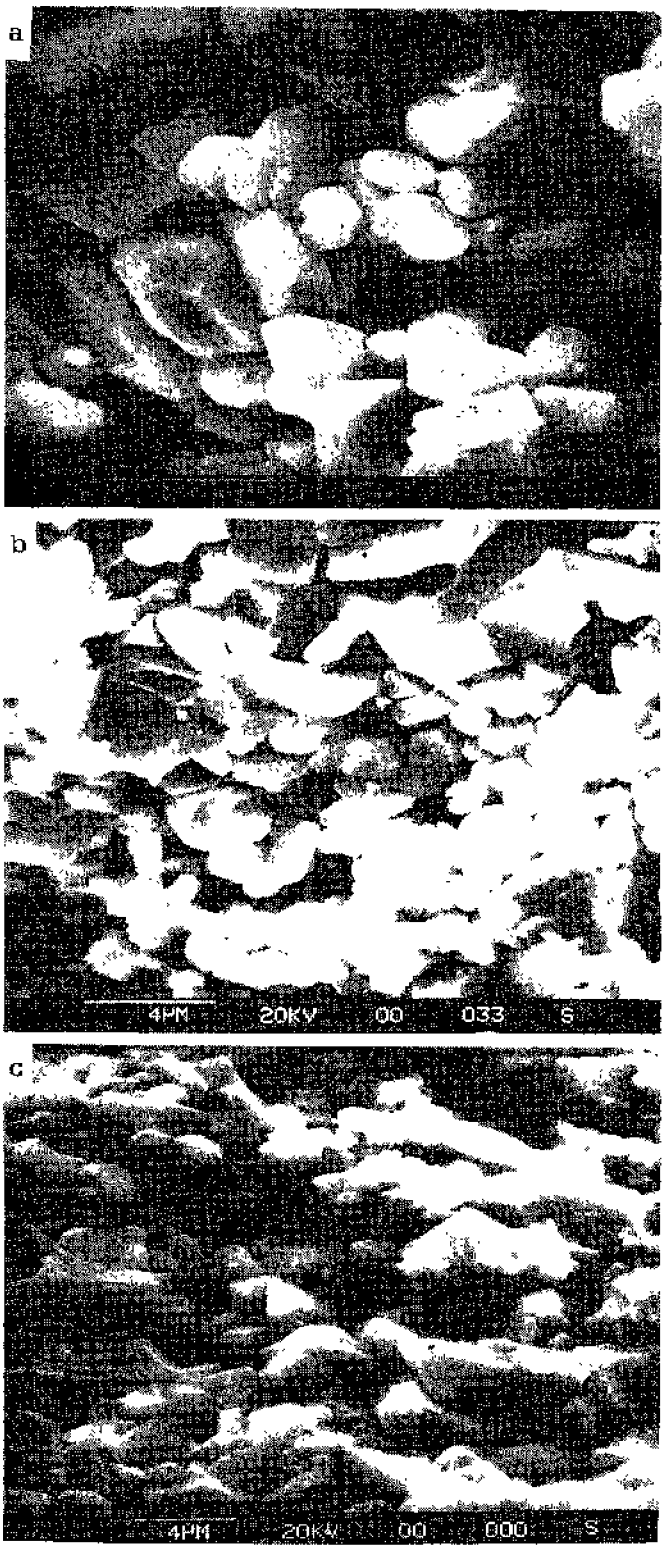

Figure 5. SEM fractographs after thermal shock test. **a**. Sample B after 5 thermal shocks. **b**. Sample C after 5 thermal shocks. **c**. Sample E after 10 thermal shocks.

than magnesia in Al_2O_3–ZrO_2 composites. Some pores were seen as black phases in the micrographs.

Figures 3a and 3b show the microstructures of compositions B and C respectively after five thermal shock treatments. Figure 3C is for composition *E* (thermal-cycled 10 times). In all these cases, grain-to-grain bonding had weakened due to thermal cycling giving rise to separation of grains or formation of microcracks with dimensions similar to the grain size. Marshall (1986) observed formation of microcracks equivalent to the grain size under load. These microcracks absorb some energy during their subcritical growth under stress (microcrack toughening). Some plasticity was developed due to this effect. Examination in back-scattered mode (Green 1982) would have clarified the microcracks better.

Although open porosity was negligible in these materials as understood from water absorption values, a lot of pores were still seen in the microstructure. This also agreed with theoretical density values shown in table 1. Because of the presence of pores, the strength values were much less. However, the presence of pores was beneficial in several applications; for example, in bioimplant, the presence of porosity was sometimes beneficial for bone growth. These materials were used as refractory materials by virtue of their good thermal shock resistance and strength.

4. Conclusions

The following conclusions are drawn from the above observations.

(i) Al_2O_3 – 29·5 wt% ZrO_2 – 1·5% Y_2O_3 composition has the highest strength and Al_2O_3 — 15 wt% ZrO_2 has a somewhat higher strength compared to Al_2O_3 – 29 wt% — 1 wt% MgO composition.
(ii) Addition of 1·5 wt% Y_2O_3 has the beneficial effect of retaining tetragonal ZrO_2 and producing fine-grained microstructure and good grain-to-grain bonding.
(iii) The increase of Y_2O_3 up to 4·5% causes formation of cubic-tetragonal-monoclinic zirconia and reduction in strength. The MgO-stabilized batch and the batch without any deliberate addition of stabilizer also had significant amount of cubic phase in addition to monoclinic ZrO_2 probably because of the impurities.
(iv) The bending strength remained the same or slightly increased in some cases after the first thermal cycling; thereafter the strength decreased abruptly on repeated thermal shock cycling, but even after 20 cycles, the samples possessed some strength.
(v) Young's modulus also decreases on thermal shock treatment up to 15th cycles, thereafter it increases. The nonlinear behaviour of elasticity or load-displacement diagram after thermal shock treatment is due to microcracks.

Acknowledgements

The authors thank Drs K K Phani, Suchitra Sen and Sri Dilip Ghosh for their kind technical assistance and Dr J Mukherji for suggestions.

References

Bansal G K and Heuer A H 1975 *J. Am. Ceram. Soc.* **58** 235
Benedetti A, Fagherazzi G and Pinna F 1989 *J. Am. Ceram. Soc.* 72 467

Buresh F E 1984 in *Advances in ceramics. Science and technology of zirconia II* (eds) N Claussen, M Rühle and A H Heuer (Columbus, Ohio; Am. Ceram. Soc.) **12** p 306
Green D J 1982 *J. Am. Ceram. Soc.* **65** 610
Heuer A H, Claussen N, Kriven W M and Rühle M 1982 *J. Am. Ceram. Soc.* **65** 642
Heuer A H, Lange F F, Swain M V and Evans A G 1986 *J. Am. Ceram. Soc.* **69** i–iv
Hori S, Yoshimura M and Somiya S 1986 *J. Am. Ceram. Soc.* **69** 169
Kibbel B W and Heuer A H 1984 in *Advances in ceramics. Science and technology of zirconia II* (eds) N Claussen, M Rühle and A H Heuer (Columbus, Ohio; Am. Ceram. Soc.) **12** p 415
Kibbel B and Heuer A H 1986 *J. Am Ceram. Soc.* **69** 231
Kosmac T, Wallace J S and Claussen N 1982 *J. Am. Ceram. Soc.* **65** C66
Lange F F and Hirlinger M M 1984 *J. Am. Ceram. Soc.* **67** 164
Lange F F and Miller K T 1987 *J. Am. Ceram. Soc.* **70** 896
Lin J T and Lu Hy 1988 *Ceram. Int.* **14** 251
Majumder R, Gilbert E and Brook R J 1986 *Br. Ceram. Trans. J.* **85** 156
Marshall D B 1986 *J. Am. Ceram. Soc.* **69** 173
Matsui M, Soma T and Oda I 1986 *J. Am. Ceram. Soc.* **69** 198
Nettleship I and Stevens R 1987 *Int. J. High Tech. Ceram.* **3** 1
Rühle M, Claussen N and Heuer A H 1986 *J. Am. Ceram. Soc.* **69** 195
Srinivasa Rao A and Cannon W R 1989 *Ceram. Intern.* **15** 179
Swain M V 1990 *J. Am. Ceram. Soc.* 73 621
Wang J and Stevens R 1988 *J. Mater. Sci.* **23** 804
Wu Xin and Chen I W 1990 *J. Am. Ceram. Soc.* **73** 746
Yuan Q M, Tan J Q and Jin Z G 1986 *J. Am. Ceram. Soc.* **69** 265
Zoz E I, Karaulov A G, Rudyak I N, Gul'ko N V and Karyakina E L 1980 *Inorg. Mater.* **16** 728